

SANDIA REPORT

SAND2002-0159

Unlimited Release

Printed January 2002

Oxidized Metal Powders for Mechanical Shock and Crush Safety Enhancers

Terry J. Garino

Prepared by
Sandia National Laboratories
Albuquerque, New Mexico 87185 and Livermore, California 94550

Sandia is a multiprogram laboratory operated by Sandia Corporation, a Lockheed Martin Company, for the United States Department of Energy under Contract DE-AC04-94AL85000.

Approved for public release; further dissemination unlimited.



Sandia National Laboratories

Issued by Sandia National Laboratories, operated for the United States Department of Energy by Sandia Corporation.

NOTICE: This report was prepared as an account of work sponsored by an agency of the United States Government. Neither the United States Government, nor any agency thereof, nor any of their employees, nor any of their contractors, subcontractors, or their employees, make any warranty, express or implied, or assume any legal liability or responsibility for the accuracy, completeness, or usefulness of any information, apparatus, product, or process disclosed, or represent that its use would not infringe privately owned rights. Reference herein to any specific commercial product, process, or service by trade name, trademark, manufacturer, or otherwise, does not necessarily constitute or imply its endorsement, recommendation, or favoring by the United States Government, any agency thereof, or any of their contractors or subcontractors. The views and opinions expressed herein do not necessarily state or reflect those of the United States Government, any agency thereof, or any of their contractors.

Printed in the United States of America. This report has been reproduced directly from the best available copy.

Available to DOE and DOE contractors from
U.S. Department of Energy
Office of Scientific and Technical Information
P.O. Box 62
Oak Ridge, TN 37831

Telephone: (865)576-8401
Facsimile: (865)576-5728
E-Mail: reports@adonis.osti.gov
Online ordering: <http://www.doe.gov/bridge>

Available to the public from
U.S. Department of Commerce
National Technical Information Service
5285 Port Royal Rd
Springfield, VA 22161

Telephone: (800)553-6847
Facsimile: (703)605-6900
E-Mail: orders@ntis.fedworld.gov
Online order: <http://www.ntis.gov/ordering.htm>



SAND2002-0159
Unlimited Release
Printed in January 2002

Oxidized Metal Powders for Mechanical Shock and Crush Safety Enhancers

Terry J. Garino
Ceramic Materials Department
Sandia National Laboratories
P.O. Box 5800
Albuquerque, NM 87123-1411

Abstract

The use of oxidized metal powders in mechanical shock or crush safety enhancers in nuclear weapons has been investigated. The functioning of these devices is based on the remarkable electrical behavior of compacts of certain oxidized metal powders when subjected to compressive stress. For example, the low voltage resistivity of a compact of oxidized tantalum powder was found to decrease by over six orders of magnitude during compaction between 1 MPa, where the thin, insulating oxide coatings on the particles are intact, to 10 MPa, where the oxide coatings have broken down along a chain of particles spanning the electrodes. In this work, the behavior of tantalum and aluminum powders was investigated. The low voltage resistivity during compaction of powders oxidized under various conditions was measured and compared. In addition, the resistivity at higher voltages and the dielectric breakdown strength during compaction were also measured. A key finding was that significant changes in the electrical properties persist after the removal of the stress so that a mechanical shock enhancer is feasible. This was verified by preliminary shock experiments. Finally, conceptual designs for both types of enhancers are presented.

Table of Contents

Introduction.....	1
Concepts for Oxidized Metal Powders Safety Enhancers.....	1
Experimental.....	3
Materials.....	3
Electrical Measurements	4
Results.....	5
Low Voltage Resistivity and Low-Stress Breakdown of As-Received Powders.....	5
Oxidation Studies.....	9
Electrical Characterization of Oxidized Powders.....	10
Breakdown of Powders after Removal of Load.....	13
Impact Studies.....	14
Discussion	15
Summary and Conclusions.....	16
Future Work.....	16
Acknowledgements.....	17
References.....	17

List of Figures

Figure 1. A conceptual design for a mechanical shock safety enhancer based on oxidized metal powders.....	2
Figure 2. SEM micrographs of the powders studied. a.) Tantalum, b.) Aluminum, c.) Titanium and d.) Silicon.....	4
Figure 3. The low voltage resistivity of tantalum powder as a function of pressure.....	6
Figure 4. The low voltage resistivity of tantalum powder as a function of density.....	6
Figure 5. The low voltage resistivity of aluminum powder as a function of pressure.....	6

Figure 6. The resistivity of the aluminum powder at low voltage during an interrupted test.....	7
Figure 7. The low voltage resistivity of the aluminum powder with and after removal of a given load.....	7
Figure 8. The low voltage resistivity of titanium powder as a function of pressure.....	8
Figure 9. The high voltage behavior of metal powders at low load.....	8
Figure 10. The TGA oxidation behavior of metal powders heated at 10°C/min in air.....	9
Figure 11. The TGA oxidation behavior of Ta powders heated at 10°C/min in air to several temperatures.....	9
Figure 12. The resistance of Ta powder during compaction at different field strengths.....	11
Figure 13. The resistance of Ti powder during compaction at different field strengths.....	12
Figure 14. The resistance of Al powder during compaction at different field strengths and with different average particle size.....	12
Figure 15. The breakdown field (where current was 1 mA) of Al and Ta powders after removal of the applied load. The load was applied at 0.5mm/min except for one Ta point that was done at 10,000 N/sec.....	13
Figure 16. Breakdown strength of silicone oil containing powders after application and removal of a load.....	14
Figure 17. The breakdown field of Ta powder oxidized at 450°C for 1 hr with silicone grease after the impact of a weight dropped from 24 cm.....	14

List of Tables

Table 1. The weight gains and estimated oxide thickness of oxidized metal powders.....	10
Table 2. The mechanical properties and estimated compaction contact stresses for Ta and Al.....	15

Introduction

The incorporation of components into a nuclear weapon that will disable it after it has been subjected to an abnormal environment enhances the safety of the weapon. Types of abnormal environments include high temperature, large mechanical shock and crushing and typically would occur as the result of an accident such as a plane or truck crash. From a nuclear safety standpoint, it is best if this component is one that is necessary for weapon detonation and that the mechanism that causes failure is the result of the fundamental laws of physics. Such a component is referred to as a weaklink. One example of a weaklink is the gel capacitor used to store the charge that sets off the detonators. The capacitor is a thermal weaklink because the weapon cannot function without it and because once it is heated above the melting point of the mylar, the melting process renders it irreversibly incapable of storing a charge.

Devising true mechanical shock and crush weaklinks has been elusive. However, components that are not true weaklinks, but, nevertheless, enhance safety, are also of value and are termed sterilizers or safety enhancers. An example of a safety enhancer would be a component connected in parallel with the gel capacitor that acts as a resistor until exposed to the abnormal environment. In the event of a mechanical shock, for example, it would become conducting, thus shorting the capacitor so it cannot hold a charge. The goal of this work was to investigate whether or not oxidized metal powders could be utilized as the active element in a mechanical shock or crush safety enhancer.

Previous work¹⁻⁴ has shown the remarkable property of certain metal powders with oxidized surfaces to decrease in resistivity by up to 7 orders of magnitude over a narrow range of increasing compressive stress. For example, a copper powder's resistance at low voltage changed from $\sim 10^6$ ohm-cm at 4 MPa to $\sim 10^{-1}$ ohm-cm at 10 MPa. In that study, the powders studied had only the thin (15 to 40 Å) native oxide layers formed at room temperature. Because of this and the fact that copper oxide is a semiconductor, not a good insulator, the copper powder compacts had relatively low breakdown fields, 145 V/cm, for example. In the present work, metals with thicker layers of insulating oxides such as tantalum and aluminum were investigated because any safety enhancer in parallel with the capacitor will have to hold off several thousand volts under normal operation without being too large (ideally 1 cm or less). Also, previous work has not looked at the electrical behavior of the powders at high voltages during compaction. This will be addressed in the present work.

Concepts for Oxidized Metal Powders Safety Enhancers

The use of an oxidized metal powder as a crush safety enhancer that would be electrically connected in parallel with a capacitor, for example, is conceptually very straightforward. The powder would be in a die press type arrangement with electrically conducting rams and a die with an insulating surface layer. The rams would be situated in such a way that they are coupled to the weapon case, and would be crushed along with it. Enough powder would be placed between the rams so that the desired amount of crushing (compressive strain) would cause the powder to no longer be able to hold off the capacitor voltage.

The use of an oxidized metal powder as a mechanical shock safety enhancer is not as simple. Two areas that need to be addressed are how to translate the shock to a compression of the powder and whether or not the shock will produce an irreversible change in electrical properties of the powder. This second issue has not been studied in previous work and will be a focus of this study, since it is critical that irreversible changes occur because the mechanical shock may well happen prior to the charging of the capacitor. To have a permanent change in the electrical properties, damage to the oxide layers at the points of interparticle contact will have to occur, as opposed to the solely electrical breakdown postulated for the copper powders that were measured during compaction.

One way to translate the mechanical shock into a compressive stress is through the use of a free mass in contact with the powder. The shock will force the free weight in the opposite direction, thus compacting the powder between the weight and the fixed container. One such conceptual design is shown in Figure 1. This design would function in response to a shock from any direction. The free mass, the metallic sphere in the center, would be one electrode and the outer spherical shell would be the other. Electrical connection to the free mass would have to be made using a feedthru to insulate it from the outer shell. A flexible wire, such as a coil, would need to be so as not to constrain the motion of the free mass. A further concern with this design is the change in density of the powder compact due to a shock. The density should not change significantly after the shock so the powder will still occupy essentially the same volume. Otherwise a large gap would open up between the compressed powder and the free mass.

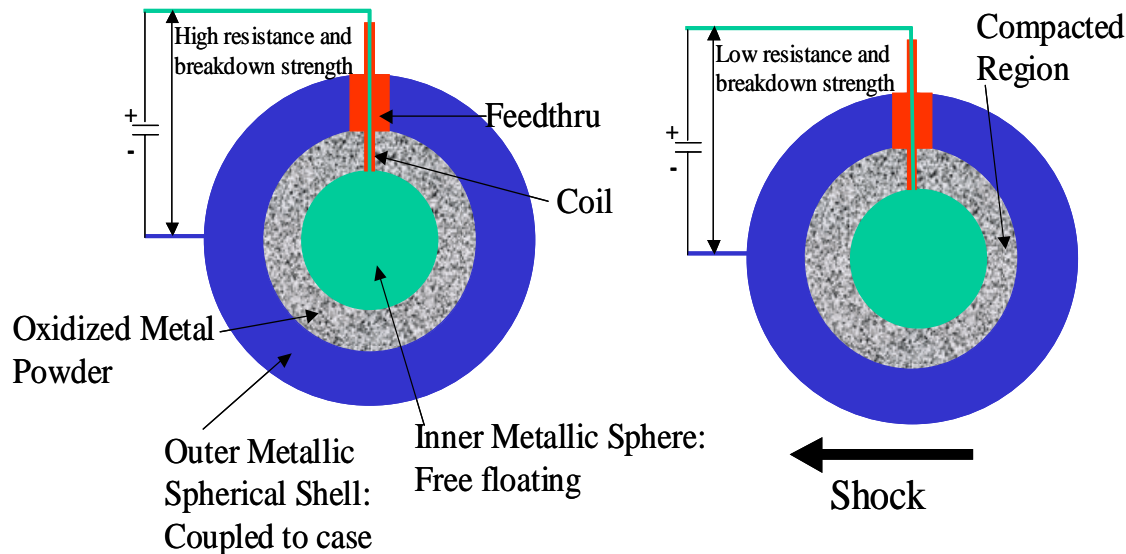


Figure 1. A conceptual design for a mechanical shock safety enhancer based on oxidized metal powders.

The stress developed due to a shock can be estimated using Newton's second law of motion, $F = m a$, where F is the force developed when a mass, m , undergoes an acceleration, a . For the geometry shown, a first order calculation of the stress generated in the powder is: $\sigma = F/\text{area} = m a/\text{area} = (\text{volume} \times \text{density}) a/\text{area} = (\rho \frac{4\pi r^3}{3}) a/\pi r^2 = \frac{4\rho r a}{3}$. For example, a 1000G acceleration on a 1 cm diameter free mass with a density of 20 g/cm³ would be: $4 (20 \text{ g/cm}^3) (1$

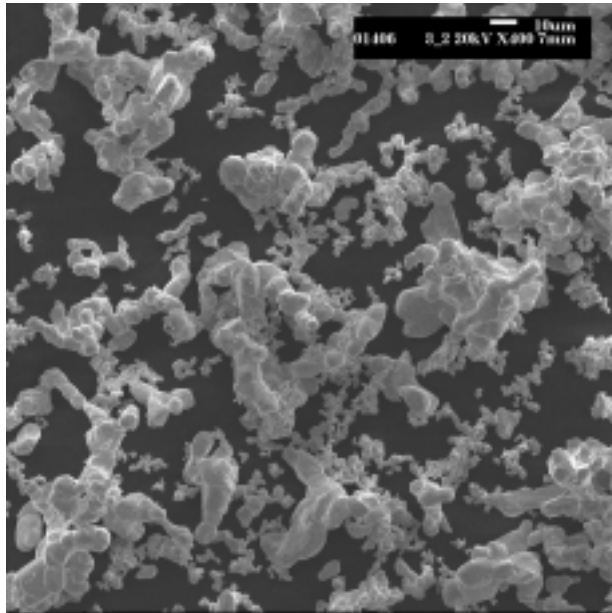
cm/2) $1000 \times 9.8 \text{ m/s}^2 / 3 \cong 1.3 \text{ MPa}$ This stress is of the same order as that shown to cause large resistivity changes in metal powders, as mentioned above.

This report summarizes the results of initial experiments designed to determine if oxidized metal powders can meet the requirements stated above. The first step was to screen some metals with oxides that are good insulators to see if their low voltage resistivity decreases during compaction, similar to copper. Then, the thermal oxidation of those metals that appeared promising, Ta, Al and Ti, was studied. The resistivity during compaction of the oxidized powders was measured at low and high voltage. Following this, electric breakdown experiments were performed on oxidized Ta and Al powders after the application and removal of a compressive stress. Next, the effects of adding binders to the powders to keep them from being free-flowing was studied. Finally, some initial shock loading tests were performed by dropping masses onto the die containing the powder, and then measuring the electric breakdown strength.

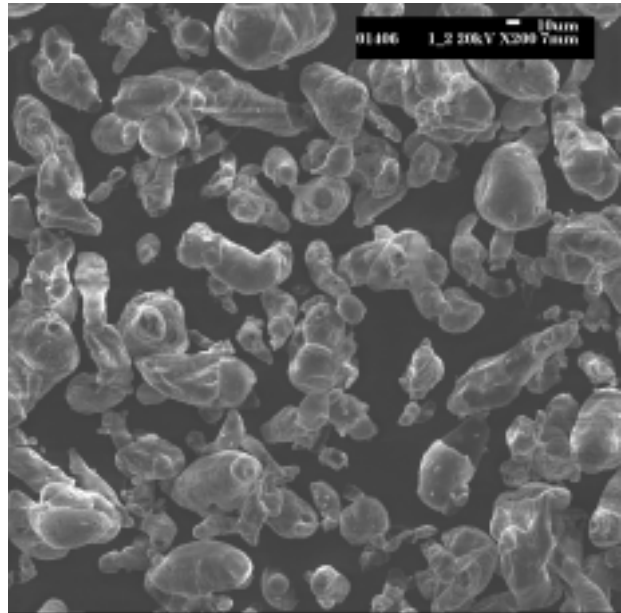
Experimental

Materials

Four metals were identified for initial evaluation because their oxides are excellent electrical insulators: tantalum ($\rho = 16.6 \text{ g/cm}^3$, 99.9%, -325 mesh, United Minerals), aluminum ($\rho = 2.7 \text{ g/cm}^3$, Fisher's Finest Powder, UN1396), titanium ($\rho = 4.5 \text{ g/cm}^3$, 99.9%, -100 mesh, Alfa Ventron, 00384) and silicon ($\rho = 2.3 \text{ g/cm}^3$, 99.999%, -60 mesh, Acros, New Jersey). Micrographs of each of the starting powders are shown in Figure 2.



a.)



b.)

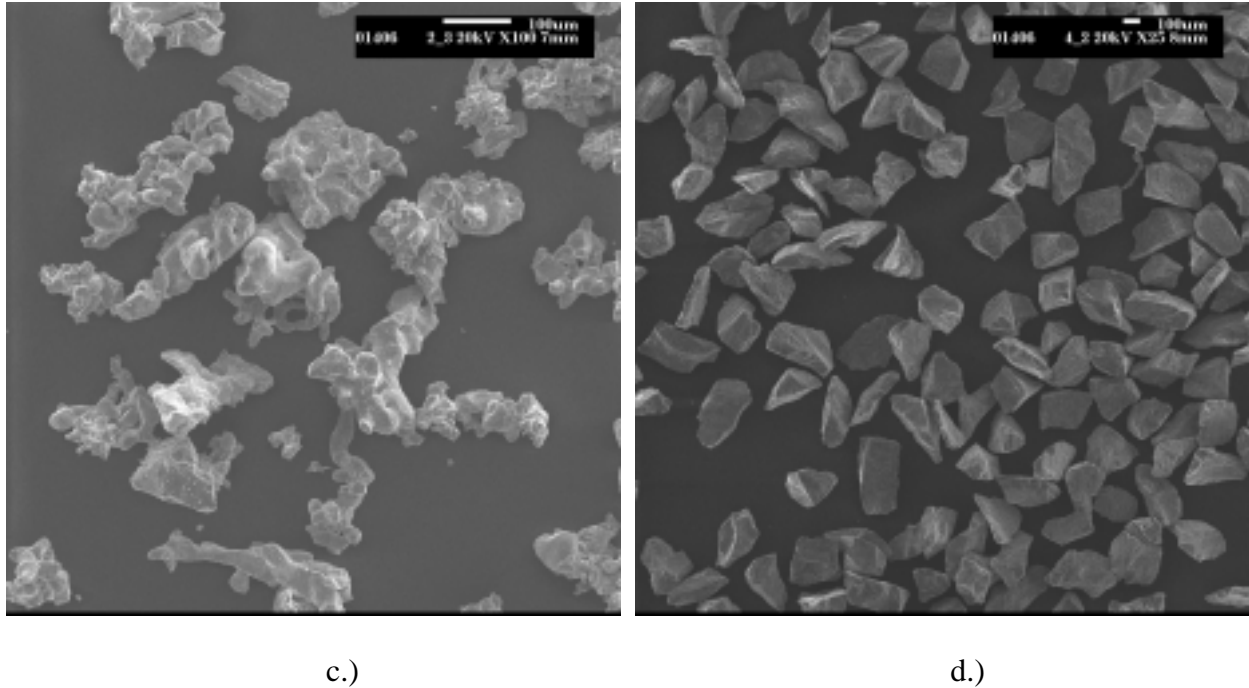


Figure 2. SEM micrographs of the powders studied. a.) Tantalum, b.) Aluminum, c.) Titanium and d.) Silicon.

The Ta powder consisted of rounded particles that appeared to be bonded together in hard agglomerates. Also, roughly 10% of the powder consisted of clusters of micron sized particles. The average particle size, from the SEM images, was $20 \pm 10 \mu\text{m}$, not counting fine particles in the clusters. The aluminum powder particles were also rounded and were agglomerated to a lesser extent than the tantalum. The average particle size was $50 \pm 25 \mu\text{m}$. The titanium powder was rounded and had large, hard agglomerates and some internal porosity. The average particle size was $139 \pm 59 \mu\text{m}$. Finally, the silicon particles were much larger and more angular and were non-agglomerated, with an average particle size of $278 \pm 50 \mu\text{m}$.

Electrical Measurements

In the first set of experiments, the low voltage resistance of the as-received powders was monitored using an ohmmeter during compaction testing from ~ 0.01 to ~ 20 MPa using a mechanical test system (MTS). The resistance, stress and strain were monitored throughout the compaction. The strain rate used was 0.5 mm/s. The powders were placed in a die with a 0.75" diameter insulating phenolic sleeve insert, and the resistance was measured between the two stainless steel rams.

Next, the electrical breakdown strength of those powders that showed promising results in the initial experiments was measured under negligible load. The same die was used but it was now connected to a high voltage power supply (High Voltage Research Inc.). The voltage was increased slowly while monitoring the current with an ammeter until a current of 1 mA was reached. The voltage at this point was defined as the breakdown voltage. The current limit on the power supply was set to 1 mA for safety reasons, since, in most cases, when breakdown occurred, the resistance decreased by many orders of magnitude.

Then, the oxidation of these powders during heating in air was studied using thermogravimetric analysis (TGA, Netzsch), since it was clear that additional oxidation would be necessary to be able to have high enough breakdown strengths at low load. The weight gain was monitored during heating at 10°C/min for all of the powders. In addition, some isothermal studies were performed on the Ta powder. The weight gain was also measured for powders that were subsequently heated and held isothermally in a box furnace. From the weight gain data, the approximate thickness of the oxide layers was calculated using a simple spherical approximation.

The breakdown tests were then repeated on a series of powders that were oxidized by heating in air at various temperatures and times. Next, the resistance of some of the oxidized powders was measured at low voltage with an ohmmeter, as well as at higher voltages using the high voltage power supply. The higher voltage measurements were done by measuring the voltage across the powder and the current flowing through it during compaction. Again, the maximum current output on the power supply was set to 1 mA.

In the next set of experiments, powders of oxidized Al and Ta were compacted under a given load using dead weights, and then the electric breakdown strength was measured using the high voltage power supply after removal of the load. Once again, the increase in current at breakdown was so abrupt in these experiments that a much higher current would have flowed if the power supply was not set at 1 mA maximum output. These experiments were also performed on powders to which various amounts of silicone vacuum grease (Dow) had been added as a weak binder. Silicone grease was chosen because of its stability and inertness. The grease was added by mixing it and the powder in hexane. The grease kept the powders from being free flowing.

In the final set of experiments, the shock response of the powders was assessed. This was done by placing the powder in the same die used for the compaction experiments and then dropping masses onto the top ram of the loading die from a distance of 24 cm. The voltage on the specimen was then increased using the high voltage power supply until breakdown occurred (the current reached 1 mA).

Results

Low Voltage Resistivity and Low-Stress Breakdown of As-Received Powders

The behavior of the low voltage resistivity of the as-received Ta powder at low voltage is shown in Figures 3 and 4 as a function of pressure and density, respectively. Figure 3 shows that the resistivity starts out very high, $>10^7 \Omega\text{-cm}$ at low pressure, and begins to decrease rapidly around 1 MPa. By 2.5 MPa, it has dropped by a factor of 1000 and by a factor of 10^6 by 6 MPa. Figure 4 shows that the density decreases only slightly as the huge change in resistivity occurs. For example, the relative density only changes by 2%, from 37% to 39%, during the initial decrease in resistivity of greater than 10^3 . This corresponds to a decrease in thickness of about 5%.

Figure 5 shows that the as-received aluminum powder behaved very similarly to the Ta. Its initial resistivity was $\sim 10^8 \Omega\text{-cm}$ up to ~ 1 MPa. It then dropped by 1000 by 4 MPa and another

1000 by 7 MPa. The dependence of the resistivity on density (not shown) was also similar to that of Ta, with a drop of about a factor of 1000 in resistivity between 48% and 50% density.

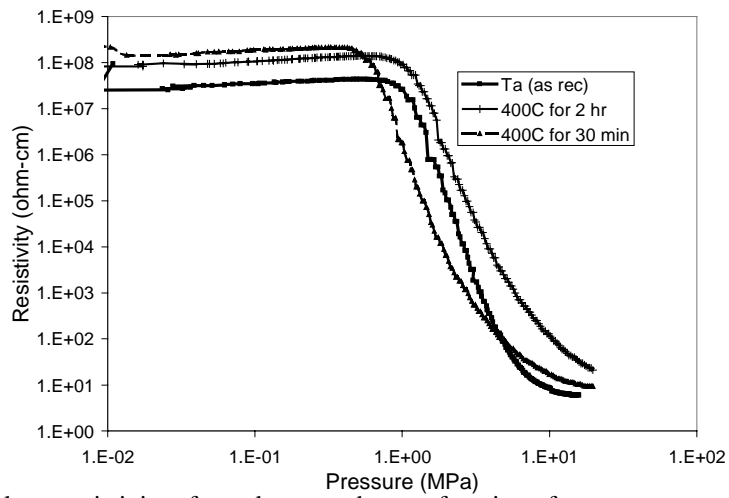


Figure 3. The low voltage resistivity of tantalum powder as a function of pressure.

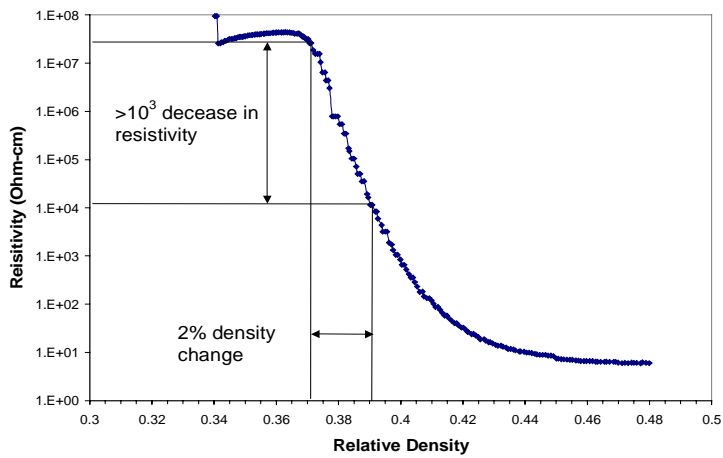


Figure 4. The low voltage resistivity of tantalum powder as a function of density.

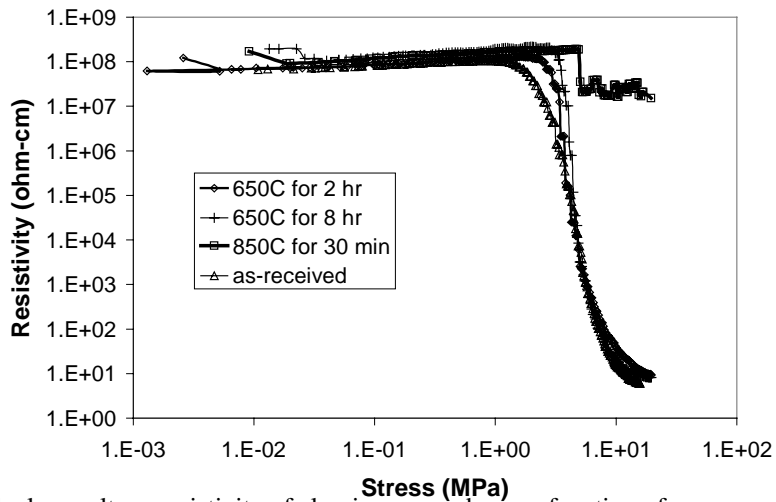


Figure 5. The low voltage resistivity of aluminum powder as a function of pressure.

Figure 6 shows the results of an interrupted test on the aluminum powder. In this experiment, the resistivity was measured while the stress was increased and then decreased before being increased to a higher level. As the figure shows, there was some recovery of the resistivity to higher values when the stress was decreased, especially at the lowest stress levels. This is shown more clearly in Figure 7 where the resistivity is plotted both with the stress still applied and after it had been removed. At loads of around 5 MPa and above the resistivity increased by a factor of ~10 after the load was removed.

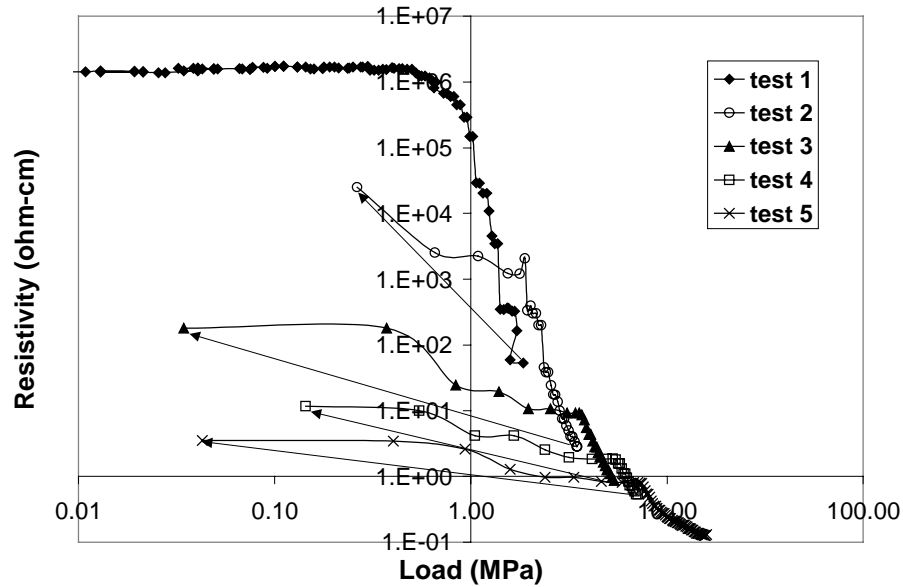


Figure 6. The resistivity of the aluminum powder at low voltage during an interrupted test.

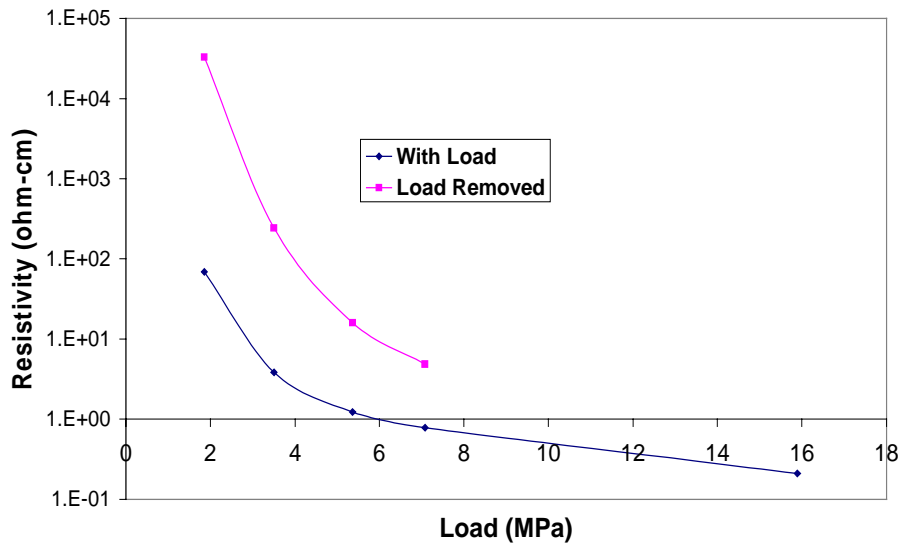


Figure 7. The low voltage resistivity of the aluminum powder with and after removal of a given load.

The as-received Si powder showed high resistivity throughout the compaction test and was therefore not considered for any subsequent testing. The behavior of the as-received Ti powder is shown in Figure 8. It was quite conducting even at the lowest loads. Therefore, oxidation of the titanium was required prior to additional testing.

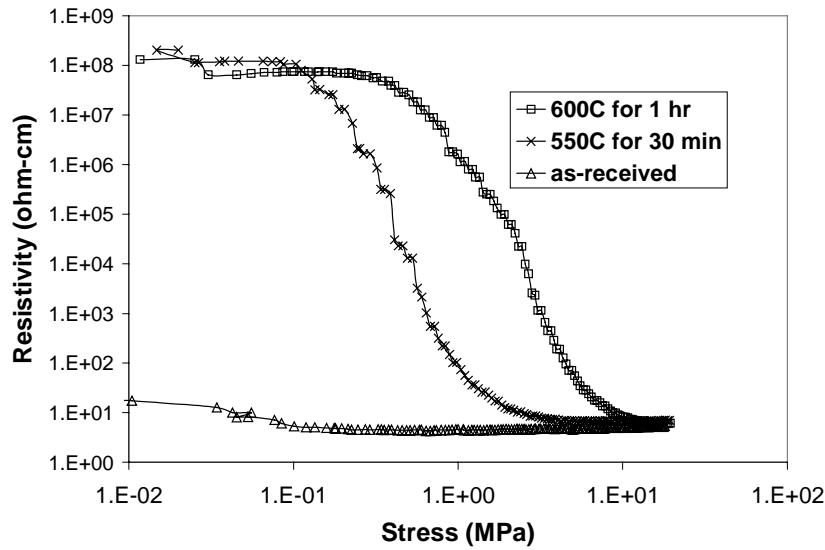


Figure 8. The low voltage resistivity of titanium powder as a function of pressure.

As mentioned above, an oxidized metal powder safety enhancer would have to be able to hold off several thousand volts without breaking down during the normal firing of the weapon. Also, to be practical, the thickness of the metal oxide powder layer in the device should be less than 1 cm. Therefore, a minimum breakdown field at low stress of 5 kV/cm is required. Therefore, the current flowing through the powders was measured as the voltage was increased until breakdown occurred (breakdown was defined as when the current reached 1 mA). The results of these measurements are shown in Figure 9, which plots the current density against the applied electric field. As the figure shows, the as-received Ta and Al powders had very low breakdown strengths so that, like the Ti, they will require oxidation if they are to be suitable for this application. Therefore, the oxidation behavior of the powders was studied next.

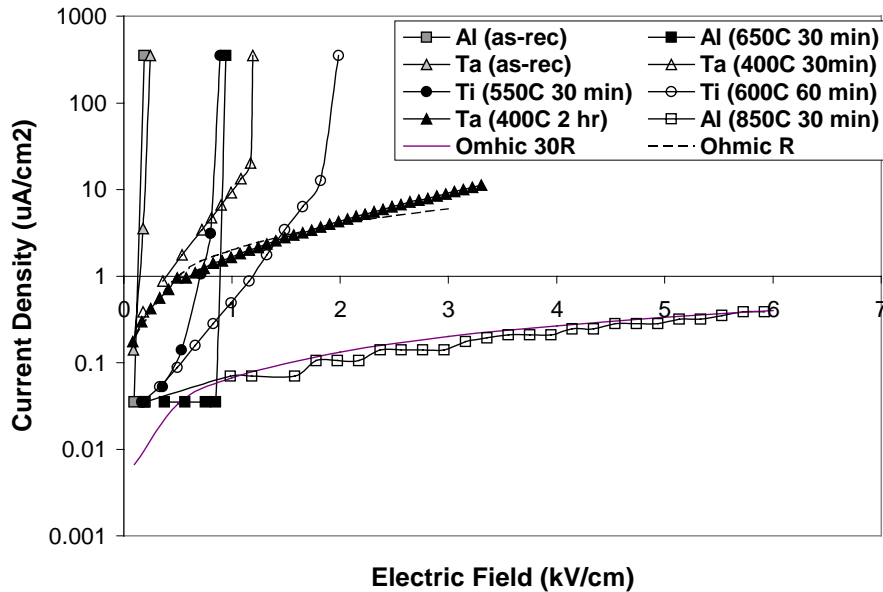


Figure 9. The high voltage behavior of metal powders at low load.

Oxidation Studies

The results of the TGA study of the oxidation behavior of the powders heated in air at 10°C/min are shown in Figure 10. The Ta starts oxidizing around 400°C, reaches a 1% weight gain by 450°C and 5% by 550°C. The Ti begins oxidizing around 500°C, reaches 1% by 600°C, and 5% by 700°C. The aluminum started to oxidize at 575°C, but did not reach 1% even at its melting point of 660°C. The results of the isothermal oxidations of Ta powder that had been size separated by sieving are given in Figure 11. The figure shows that at 400°C, the 3 coarsest cuts behaved similarly. The finest, -10 μm, oxidized somewhat more, as would be expected due to its higher surface area. Also, the rate of oxidation at 500°C was much greater than at 450°C for the 10 to 20 μm powder. Based on these results, oxidation conditions were chosen for the powders to produce weight gains in the range of a few percent. Table 1 gives the measured weight gains for each of the oxidized powders for all the oxidation conditions used along with an estimate of the thickness of the oxide layer. The oxide thickness was calculated assuming spherical particles with average size determined from the micrographs in Figure 2, also given in the table. The calculated oxide thickness for the powders is between 0.18 and 0.65 μm.

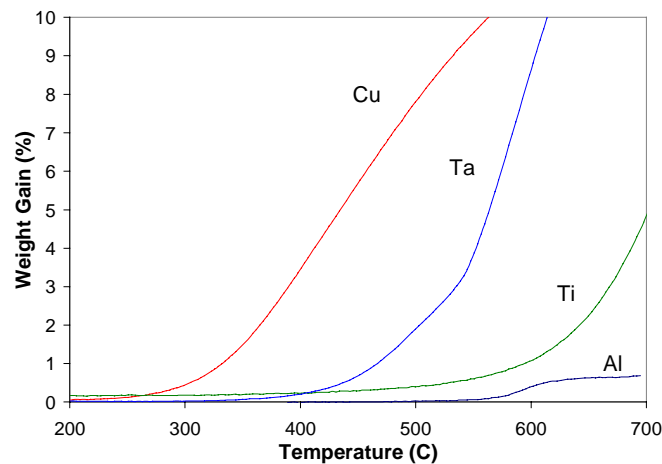


Figure 10. The TGA oxidation behavior of metal powders heated at 10°C/min in air.

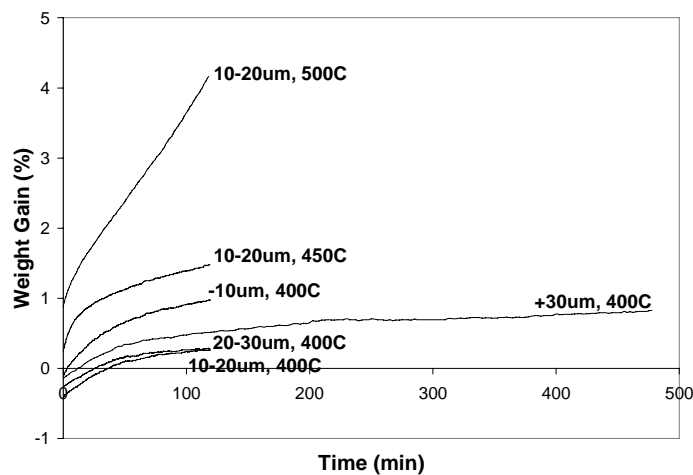


Figure 11. The TGA oxidation behavior of Ta powders heated at 10°C/min in air to several temperatures.

Table 1. The weight gains and estimated oxide thickness of oxidized metal powders.

Powder	Ave. Particle Size (μm)	Temperature ($^{\circ}\text{C}$)	Time (hr)	Weight Gain (%)	Degree Oxidized (%)	Oxide Thickness (μm)
Aluminum	50	650	0.5	0.73	0.8	0.18
Aluminum	50	650	2	0.79	0.87	0.19
Aluminum	50	650	8	1.0	1.1	0.24
Aluminum	50	850	0.5	2.7	3.0	0.65
Tantalum	20	400	0.5	0.46	2.1	0.34
Tantalum	20	400	2	0.62	2.8	0.46
Titanium	139	550	0.5	0.47	0.7	0.29
Titanium	139	600	1	0.94	1.4	0.57

The Electrical Characterization of Oxidized Powders

The current density versus field at negligible stress (weight of top die ram only) of Ta oxidized under two different conditions is shown in Figure 9. After 30 min at 400°C ($0.34\ \mu\text{m}$ thick oxide), the breakdown field increased to $\sim 1.2\ \text{kV/cm}$, whereas after 2 hr at 400°C ($0.46\ \mu\text{m}$ thick oxide) the sample did not breakdown up to $\sim 3.3\ \text{kV/cm}$, where the test was stopped. Also shown on the graph is a curve for the behavior of an ideal ohmic resistor that closely matched that of the 2 hr sample, indicating that it is behaving linearly. The breakdown strength of Ta_2O_5 made by DC magnetron sputtering has been reported to be several MV/cm .⁵ This is much higher than what was measured for the oxidized Ta powders even after accounting for the enhancement⁶ of the electric field by $1.5\ r/t$, where r is the particle radius and t is the oxide thickness, due to the fact that the interior of the particles is conducting. With this enhancement, the breakdown field for the powder held for 2 hr at 400°C is still only $72\ \text{kV/cm}$. However, this is not surprising for several reasons. First, the breakdown strength of oxides increases as the thickness of the sample decreases due to the presence of defects so that bulk samples may breakdown at fields 100 times or more lower than a thin film. Also, the fact that the particles are not perfect spheres but have aspersions also contributes to the lower breakdown strength.

The low voltage resistivity of these oxidized powders during compaction is shown in Figure 3. The low load resistivity of both oxidized powders was somewhat higher than that of the as-received powder. Both oxidized powders underwent the same sharp decrease in resistivity. The 30 min sample decreased at a slightly lower load than the as-received powder and the 2 hr at a slightly higher.

Two oxidation conditions for the Al powder are also shown in Figure 9. A 650°C for 30 min treatment ($0.19\ \mu\text{m}$ thick oxide) increased the breakdown field to nearly $1\ \text{kV/cm}$. The sample heated to 850°C for 30 min ($0.65\ \mu\text{m}$ thick oxide) did not break down up to $6\ \text{kV/cm}$, where the test was stopped. It also behaved linearly as shown by the curve. Its resistivity was about 30 times greater than that of the best Ta powder. Due to the protective oxide coating, this powder

remained a powder even though it had been heated to nearly 200°C above its melting point. However, the corrected breakdown strength, >350 kV/cm for the sample heated to 850°C, was still well below the value of 11 MV/cm that has been reported for a thin film.⁷

The low voltage resistivity of oxidized Al powders during compaction is shown in Figure 5. The curves for the two times at 650°C, 30 min and 8 hr (1.0% weight gain), are very similar to that of the as-received powder except that the onset of the drop in resistivity occurs at a higher stress in the oxidized powders, making for an even sharper drop in resistivity. The powder heated to 850°C remained insulating even at the highest pressure.

Two oxidation conditions were used for the Ti powder. After 30 min at 550°C (0.47% weight gain), the breakdown field increased to about 1 kV/cm. After an hour at 600°C (0.94% weight gain) it increased to about 2 kV/cm. In both cases, the behavior was non-ohmic, with the resistivity decreasing with increasing field. The low voltage resistivity of these powders during compaction is shown in Figure 8. The low stress and high stress resistivities of both powders are nearly identical, 10^8 and $10 \Omega\text{-cm}$, respectively. However, the 550°C powder began to decrease in resistivity at ~ 0.1 MPa, as opposed to ~ 0.5 MPa for the other powder.

Oxidized powders of Ta, Ti and Al were then compacted using the mechanical testing system while a higher, constant voltage was applied. The resistivity was determined from the current flowing through the sample that was measured with an ammeter. Initial field strengths of 0.53 and 1.06 kV/cm were used, and the fields increased slightly during compaction as the separation between the plungers decreased. Figure 12 shows the results for Ta. A sharp decrease in resistivity occurs at a stress that is at least an order of magnitude lower at the higher fields than at low field, below 0.1 MPa for the powders oxidized for 1 hr. It also shows that the less oxidized powder breaks down at a lower stress than the powder oxidized for 2 hr, as expected. Also, for powders that were oxidized the same, the higher field produced a decrease in resistivity at lower stress levels.

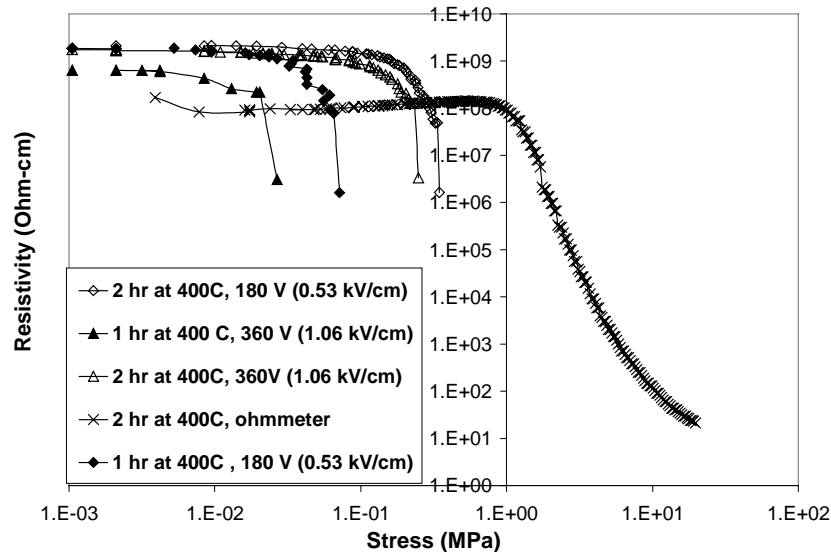


Figure 12. The resistance of Ta powder during compaction at different field strengths.

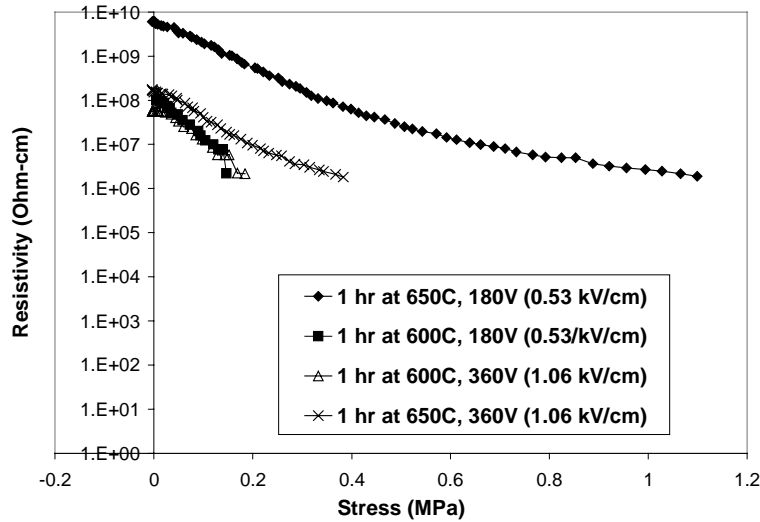


Figure 13. The resistance of Ti powder during compaction at different field strengths.

Figure 13 shows that the behavior of the Ti powder was very different from that of the Ta as it did not show a sharp resistivity drop. Because of this result, the Ti was not studied further.

Figure 14 shows the results of the high voltage compaction measurements for the Al powder that was heated to 650°C for 8 hr. As with the Ta, the decrease in resistivity was both sharper and at lower stress than at low voltage (compare to Figure 3). Also shown are results for the same powder heated to a slightly lower temperature and then size separated using sieves. In this case, the smallest size cut of the powder, less than 25 microns, required a higher stress to produce the resistance drop, almost 2 MPa, than the other two, which were around 1 and 0.5 MPa for the 25 to 38 micron and the greater than 38 micron cuts, respectively. This was most likely due to the fact that the smaller particles were more oxidized than the larger particles due to their higher surface area.

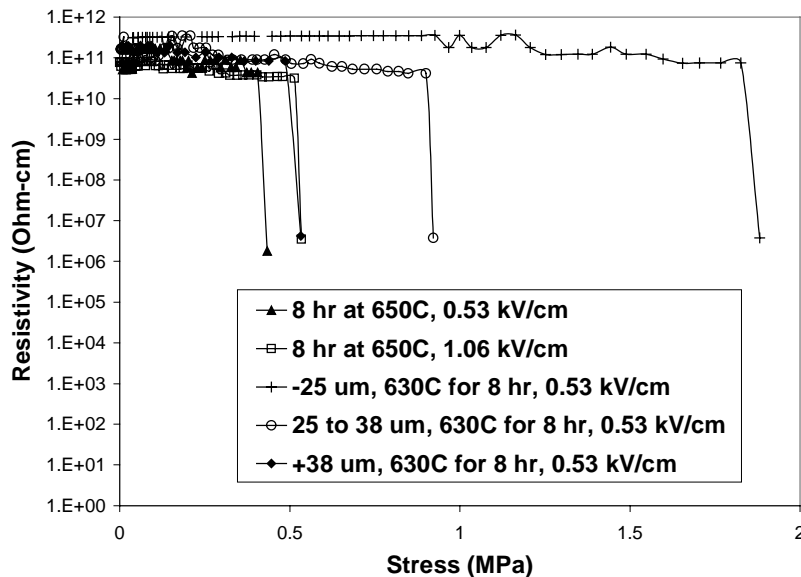


Figure 14. The resistance of Al powder during compaction at different field strengths and with different average particle size.

Breakdown of Powders after Removal of Load

Since both the Ta and the Al thermally oxidized powders behaved in the desired manner during compaction at higher field, they were both studied in a set of experiments where the breakdown field was measured after the application and removal of a stress. This is important for a mechanical shock safety enhancer application since the capacitor may not begin to charge until some time after the shock. The results of these experiments are shown in Figure 15. The initial breakdown field at low stress (weight of upper die ram only) for both metal powders tested, Ta that had been heated to 400°C for 2 hr and Al that had been heated to 700°C for 8 hr, was right at 5 kV/cm. This is right at the minimum requirement mentioned above. The Ta powder showed a lasting decrease in breakdown field after stresses in the 0.1 to 2 MPa range were applied. The breakdown field for the Ta decreased rapidly with stress, such that it went from nearly 5 kV/cm to 1 kV/cm at 0.25 MPa. When the load is plotted on a log scale, the decrease in breakdown field for Ta was linear. Also, one data point was taken at a high loading rate, 10,000 N/s, as opposed to the lower rate of 0.5 mm/min used for the rest of the data. A significant decrease in breakdown field occurred even at this high loading rate, although it was not as much as at the slower rate. This result indicated that the effect may be very similar during shock loading, since that also occurs over a short time period. Also, in all of the breakdown tests, the resistivity of the powder remained low once breakdown had occurred even if the voltage was decreased to a few volts. However, if the powder was mixed with a spatula, it returned to its initial high resistivity state.

The results for the Al powder were somewhat different. Only a slight decrease in breakdown strength was seen out to about 0.75 MPa (from about 5 to about 3.6 kV/cm). However, by 1 MPa, the breakdown field had decreased to <2kV/cm. At higher stresses the breakdown field unexpectedly began increasing.

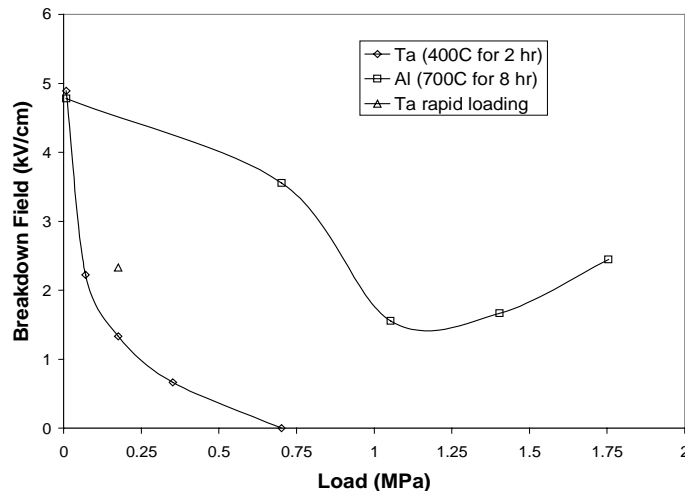


Figure 15. The breakdown field (where current was 1 mA) of Al and Ta powders after removal of the applied load. The load was applied at 0.5mm/min, except for one Ta point that was done at 10,000 N/sec.

A similar experiment was performed on a Ta powder that had been oxidized at 400°C for 2 hr to which silicone oil had been added (0.666 g of oil to 10 g of Ta). The results of the experiments are shown in Figure 16. Even with the oil present, there was a significant decrease in the

breakdown strength of the powder at stresses well below 1 MPa. Although the oil did not impart any great strength to the compacted powder, it did prevent the powder from being free flowing.

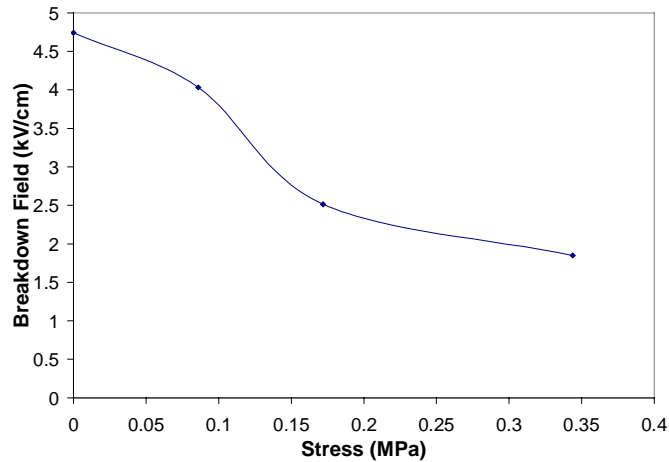


Figure 16. Breakdown strength of silicone grease containing powders after application and removal of a load.

Impact Studies

A number of initial impact studies were performed on the powders. In these studies a metal mass was dropped onto the die from a height of 24 cm and the breakdown field was then measured. The results of one such test are shown in Figure 17 for a silicone grease containing oxidized Ta powder (450°C for 1 hr). The breakdown field, which in this case was over 12 kV/cm initially, decreased with the mass of the weight that was dropped to around 6 kV/cm for a 200 g weight. These results indicate that it may be possible to use oxidized metal powders as shock safety enhancers, since a large decrease in breakdown field occurs in response to an impact. The actual acceleration imparted to the top ram by the falling weights has not been measured, but is thought to be in the kilo-g range. Further testing with known accelerations are needed to quantify this effect.

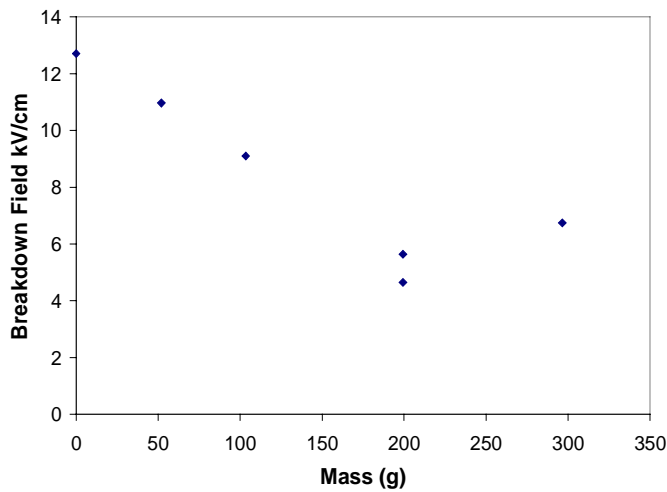


Figure 17. The breakdown field of Ta powder oxidized at 450°C for 1 hr with silicone grease after the impact of a weight dropped from 24 cm.

Discussion

To understand the origin of the effects studied here, the details of what occurs to metal particles during compaction must be understood. When a powder is compacted, the contact regions between the particles along the direction of compaction experience a much higher level of stress than the nominal applied stress because the area of contact is generally much smaller than the particle size. Hertz^{8,9} analyzed the problem of an elastic sphere in contact with a flat surface over 100 years ago. Although this is not the same geometry that exists when irregularly shaped particles are compacted, Hertzian analysis can be done to estimate the stress levels at interparticle contact points in a compacting powder. The actual stresses will probably be somewhat lower due to frictional forces and particle rearrangement. According to Hertz, the radius of contact between a sphere and a plate of the same material is given by

$$a = \{3PR(1-\nu)^2/(2E)\}^{1/3} \quad (1)$$

where P is the load on the sphere of radius R , and ν and E are the Poisson's ratio and Young's modulus of the material. The load on each particle contact in a die filled with powder can be approximated as

$$P = P_a(R/R_d)^2 \quad (2)$$

where P_a is the load applied to the die of radius R_d . Finally, the compressive stress on each contact is just the load over the contact area

$$\sigma_c = P/(\pi a^2) = P_a^{1/3}/\{\pi[3R_d(1-\nu)^2/(2E)]^{2/3}\} \quad (3)$$

after substitution of Equations 1 and 2.

The mechanical properties of tantalum and aluminum are given in Table 2. These were used in Equation 3, along with $P_a = 50$ N (~ 5 kg) and $R_d = 0.95 \times 10^{-2}$ m (nominal stress = 0.18 MPa), to give the contact stress values also given in the table. As the table indicates, the contact stress for each metal is well above its yield stress. This means that significant plastic deformation is taking place at the contact areas, even at very low nominal stress values well under 1 MPa.

Table 2. The mechanical properties and estimated compaction contact stresses for Ta and Al.¹⁰

Material	Young's Modulus (GPa)	Poisson's Ratio	Contact Stress (GPa)	Yield Stress (hard, GPa)
Tantalum	185.7	0.342	1.13	0.760
Aluminum	70.6	0.345	0.60	0.11-0.17

When this plastic deformation occurs, the thin oxide layer on the surface of the particles must crack in the contact regions thus allowing some metal-to-metal contact where the cracks in the oxide on the two particles overlap. Even if there is not direct metal-to-metal contact, when the oxide cracks a conducting path can be formed by mobile species such as water on the surface of

the oxide. Once conduction takes place between two particles, the voltage drop on the remaining contacts increases, giving rise to the abrupt breakdown of the entire sample.

With this understanding, the results presented in this report can be explained. For example, as an oxidized metal powder is compacted, more and more contact points reach a stress level where the oxide cracks and allows metal-to-metal contact or close proximity, thus lowering the resistivity. The breakdown strength at each contact point will depend on the distance between the exposed metal surfaces. This is why when the testing is done at higher voltage, breakdown occurs at even lower stress levels, since the higher fields can cause breakdown at contacts where the cracks are smaller and further separated. Obviously, the thicker the oxide, the harder it will be to crack and the wider the gap between the exposed metal surfaces. That is why, in general, the stress or field required for breakdown increased with the amount of oxide. This also explains the results of the interrupted test in Figure 6 and 7: when the stress is removed, the gaps between the particles slightly widen thus increasing the resistivity. Finally, it also explains why mixing a powder that had been broken down restores it to its original high resistivity state since the network of interparticle contacts is destroyed by the mixing.

Summary and Conclusions

In conclusion, this report shows that oxidized metal powders can meet the requirements for use in crush and mechanical shock safety enhancers. Two metals, tantalum and aluminum, were found to have the best properties of the metals studied for this application. When appropriately oxidized, they were able to hold off >5 kV/cm and still decrease in low voltage resistivity by three orders of magnitude over a range of several MPa starting around 1 MPa. The behavior of these powders during compaction at higher voltage showed that they undergo an abrupt breakdown at even lower levels of stress, in the range of 0.1 MPa. These results indicate that the use of these powders in crush applications is relatively straightforward. In addition, a significant decrease in the breakdown field was demonstrated for these metals, even after the removal of the stress and after an impact load was applied. The results of these experiments indicated that the breakdown strength of both metals decreased significantly when stresses as low as 0.2 MPa were applied and removed. This result confirms that oxidized metal powders may be suitable in mechanical shock applications where the voltage may not be applied until after the shock has occurred. However, one possible barrier to their use in shock applications is that some compaction of the powder does occur in response to a shock that might create an air gap between the powder and one of the electrodes. The presence of such a gap may keep the enhancer from functioning properly. Finally, these results were explained by proposing that the contact stresses between the particles crack the insulating oxide coating so that the metal surfaces are either separated by a narrow gap or are in direct contact.

Future Work

There are three areas where further work is warranted. The first is to better understand the mechanism responsible for the cracking of the oxide layers, by performing experiments on either single particles or wires. These could be put in contact with a known force and separation, possibly using a nano-indenter, while a voltage is applied and the current flow measured. The contact surfaces could then be examined using an SEM to see what type of damage occurred.

This will give a better understanding of the force needed for cracking, and provide insight on how the breakdown voltage varies with force and separation. The second area for more research is to try to further optimize the powders for these applications by doing similar experiments to those reported here. Also, additional experiments, such as calibrated acceleration or impact testing, should be performed. Finally, building and testing of prototype devices should begin to fully validate this concept.

Acknowledgements

The author wishes to express his gratitude to Clay Newton, Dale Zscheishe, Walter “Chip” Olson, Marlow Weston, Gary Zender and Michael Howard for their technical assistance, to Aaron Hall and Ken Eras for helpful discussions, and to Bruce Tuttle for his guidance in making the high voltage electrical measurements. This work was performed at Sandia National Laboratories. Sandia is a multiprogram laboratory operated by Sandia Corporation, a Lockheed Martin Company, for the United States Department of Energy under Contract DE-AC04-94AL85000.

References

1. K.-J. Euler, P. Herger, H. Metzendorf and B. Sperlich, “Electric Conductivity of Compressed Copper Powder. Aging and Influence of Electric Field Strength,” *Powder Technology*, **27**, 53-59 (1980).
2. K.-J. Euler, R. Kirchhof, and H. Metzendorf, “The Electric Conductivity and Related Phenomena of Compressed Metal Powders,” *Materials Chemistry*, **4**, 611-630 (1979).
3. R. Kirchhof, “The Particle Shape Influence on the Apparent Density and Electric Conductivity of Pressed Powder Materials,” *Materials Chemistry*, **6**, 209-222 (1981).
4. B. Sperlich, “The Electric Conductivity of Mixed Copper and Nickel Powders,” *Materials Chemistry*, **5**, 169-184 (1980).
5. J.Y. Kim, M.C. Nielsen, E.J. Rymaszewski, T.M. Lu, “Electrical Characteristics of Thin Ta₂O₅ Films Deposited by Reactive Pulsed Direct-Current Magnetron Sputtering,” *Journal of Applied Physics*, **87**, 1448-1452 (2000).
6. R.A. Anderson, “Effects of Finite Conductivity on Electrorheological Fluids,” pp. 81-92 in **Electrorheological Fluids: Mechanisms, Properties, Structures, Technology and Applications**, R. Tao, ed., World Scientific, Singapore, 1992.
7. N.P. Magtoto, C. Niu, B.M. Ekstrom, S. Addepalli, J.A. Kelber, “Dielectric Breakdown of Ultrathin Aluminum Oxide Films Induced by Scanning Tunneling Microscopy,” *Applied Physics Letters*, **77**, 2228-2230 (2000).
8. B.R. Lawn and T.R. Wilshaw, **Fracture of Brittle Solids**, Cambridge University Press, Cambridge, 1975, p19-20.
9. H. Hertz, **Hertz’s Miscellaneous Papers**, MacMillan, London, 1896, ch. 5-6.
10. Goodfellow Corp. Catalog, Berwyn, PA, 2000.

Distribution for SAND Report "Oxidized Metal Powders for Mechanical Shock and Crush Safety Enhancers," by T. J. Garino

MS-1411 D. Tallant, 1822
MS-0889 G. Knorovsky, 1833
MS-0889 A. Hall, 1833
MS-0889 R. Anderson, 1843
MS-1411 T. Garino, 1843 (5)
MS-1349 K. Ewsuk, 1843
MS-1349 W. Hammetter, 1843
MS-1349 J. Cesarano, 1843
MS-0889 S. Glass, 1843
MS-0889 C. Newton, 1843
MS-1411 B. Tuttle, 1843
MS-0888 K. Rahimian, 1846
MS-0319 K. Eras, 2613
MS-0319 R. Kreutzfeld, 2613
MS-0885 G. Heffelfinger, 1801
MS-0885 D. Dimos, 1802
MS-0887 M. Cieslak, 1800
MS-9018 Central Technical Files, 8945-1
MS-0899 Technical Library, 9616 (2)
MS-0612 Review and Approval Desk, 9612